

Semiconductive Cellulose Nanocrystal-Polyfluorene Emissive Material in OLEDs

Allen C. Chang, M. Bachir Messikh, Maximilian Kaiser, Kenneth R. Carter*

Department of Polymer Science and Engineering, University of Massachusetts Amherst, 120 Governor's Drive, Amherst, MA, 01003.

KEYWORDS: *Cellulose Nanocrystals (CNC), Polyfluorene, OLED, Surface Modification*

ABSTRACT: Cellulose nanocrystals (CNCs) were functionalized with aryl bromides moieties and subsequently grafted with a semiconducting polyfluorene. A straightforward Yamamoto type cross coupling polymerization was employed to graft chains of poly (9,9-dihexylfluorene) from surface bound aryl halides. These composite materials, g-PFCNC, exhibit polyfluorene graft lengths with average $M_w \sim 4000$ Da. Organic light emitting diodes (OLEDs) were fabricated on ITO/glass substrates using g-PFCNC as the active emissive layer. These devices have a turn on voltage (V_{on}) of ~ 4.5 V and emit in the blue frequency characteristic of homopolyfluorene. The active layer is non-uniform, contains upwards of 85 wt% cellulose, and is fabricated, in large part, outside of an inert atmosphere. The results of this work push forward a new family of sustainable cellulose-based devices.

Advancements in sustainability have been made across a myriad of technologies, especially in the sectors of renewable energy, energy storage, and electronics¹⁻⁴. Solar cells have been increasing in efficiency for decades while the associated library of useful materials has grown extensively⁵⁻⁸. Organic field effect transistors have seen marked improvements⁹ accompanied by movements toward paper-based systems¹⁰⁻¹³. The field of organic light emitting diodes has seen some push toward sustainability, namely in utilizing cellulosic substrates for flexible OLEDs¹⁴⁻¹⁶. A unique opportunity that has been less explored is the incorporation of renewable materials in the actual active layers of organic electronics¹³. Based off previous works which have explored grafting of polymers from nanocellulose thru ring opening and ATRP¹⁷⁻²¹, composite materials may combine the mechanical properties of a cellulosic substrate material²²⁻²⁵ with the electrical conductivity and emissive properties of polyfluorene active materials²⁶⁻³⁶. Furthermore, the use of cellulose materials paves the way for more sustainable and environmentally friendly device fabrication. Such breakthroughs will result in future concepts such as an all paper OFETs and OLEDs. However, efforts in this area have been stymied by a lack of exploration in novel composite materials. Few researchers^{13,30,37,38} have explored the necessary grafting chemistries for cellulose-conjugated polymer synthesis.

Herein we describe the synthesis and fabrication of an electronically active composite layer containing cellulose nanocrystals (CNCs), a material well-known as a sustainable strengthening additive, and conjugated poly(9,9-dihexyl fluorene), a well-known blue emitter. Grafted cellulose nanocrystal-polyfluorene composites (g-

PFCNCs) were synthesized through a series of processing steps starting with a solvent exchange of CNC into toluene, followed by a surface modification with an aryl bromide (Figure 1a), and ending with a Yamamoto cross coupling graft polymerization (Figure 1b).

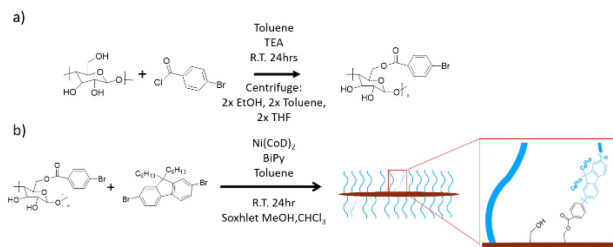


Figure 1. General synthesis pathways for a) CNC surface aryl halide functionalization thru acid chloride esterification and b) Yamamoto graft polymerization of polyfluorenes from modified CNCs.

Solvent exchange was performed through a series of centrifugation and redispersion steps starting by dripping an aqueous dispersion of CNCs in water (11.8 wt%) into acetone. After centrifugation for 30 minutes at 4500 RPM, the acetone was poured off, fresh acetone was added and the CNCs re-dispersed via sonication and mechanical agitation. This process was repeated 3 times through acetone, toluene, and finally anhydrous toluene. NMR analysis of the final toluene solution showed approximately 1% of water after all solvent exchange was complete. Subsequently, a surface modification with 4-bromobenzoyl acid chloride was performed^{30,37}, yielding CNC with ester bonded surface aromatic bromine groups (s-BRCNC). Polymer grafts were grown from the surface halides via Yamamoto cross coupling methods using a

fluorene monomer. S-BRCNC in toluene was grafted with 2,7-dibromo-9,9-dihexyl fluorene using stoichiometric amounts of $(CoD)_2Ni(o)$ and bipyridine as the cross coupling agents. Reactions were carried out under inert atmosphere at $50^\circ C$ overnight. Side products were washed out through successive rinsing and centrifugation steps.

Resulting g-PFCNC materials exhibited graft lengths well above the effective conjugation length ($n > 10$) of polyfluorene, signaling an expected consistency in grafted polymer properties. Any grafts shorter than the effective conjugation length could have a range of properties including blue shifted UV absorption maximum and lowered emissive capabilities. Due to the inherent insolubility of the final CNC product, the PF grafts were cleaved from the CNC by acid hydrolysis of the ester linkage. The PF was separated from the CNC and characterized via MALDI-ToF spectroscopy and UV-Vis. Homopolymer side product and the grafted products showed comparable molecular weights and absorbance maxima (Figure 2). When compared with literature values^{28,32,35}, the absorbance maxima observed aligned with those seen in polymeric chains of polyfluorene, saturating around 385 nm. Additionally, when compared to our first reported Sonogashira grafting study³⁰ using poly (2-ethynyl-9,9-dihexyl fluorene) which showed grafts of $M_w \sim 1000 - 2000$ Da and absorbance at 350 nm, Yamamoto grafting yields polymers ($M_w \sim 4000$ Da) that are up to 4x longer and absorb at normalized maximum of 366 nm with a leading shoulder above 370 nm.

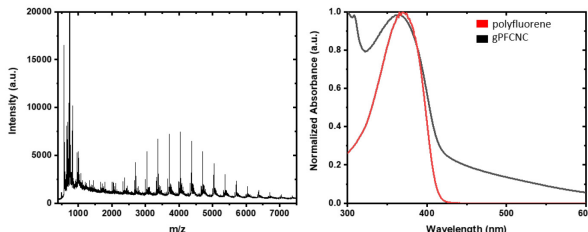


Figure 2. MALDI-ToF spectrum of g-PFCNC (Left) and normalized UV-Vis (Right) of g-PFCNC (black) and PF (red).

After establishing the procedure for synthesizing g-PFCNC, we confirmed its electroluminescent properties by fabricating OLED devices. Top contact OLEDs were made using conductive ITO/glass substrates, PEDOT:PSS electron transport layer, g-PFCNC active layer, poly (4-n-hexyl-triphenyl)amine (HTPA) electron blocking hole transport layer, and Ca/Al contacts (Figure 3). ITO substrates were first sonicated in 2-propanol for 10 minutes, dried under a stream of N_2 , then cleaned under UV/Ozone exposure. A PEDOT:PSS solution (45 μL) was spin coated on the ITO surface at 4000 RPM for 30 seconds then baked at $120^\circ C$ for 10 minutes. Subsequently, 30 μL g-PF-CNC (5mg/mL) in $CHCl_3$ was spin coated at 3000 RPM for 30 seconds and allowed to dry, followed by 30 μL of HTPA with the same spin coating procedures. The HTPA coated substrate was heated for 30 minutes at $80^\circ C$. Polyfluorene based OLEDs were also prepared as standards to compare against the g-PFCNC devices. These standard devices were made with the same overall structure

substituting polyfluorene homopolymer as the active layer and not using the HTPA layer.

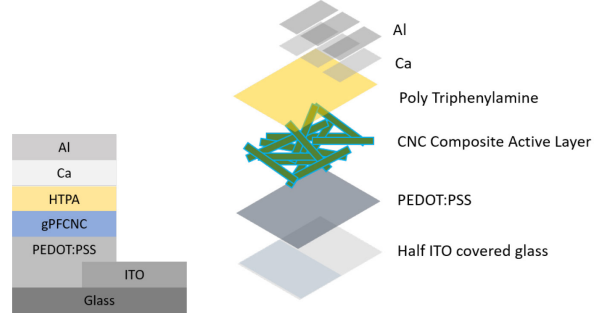


Figure 3. Composite material OLED device structure.

The I-V curves for the devices are shown in Figure 4. Both polyfluorene and g-PFCNC OLEDs operate in a comparable fashion. The composite g-PFCNC OLEDs exhibit diode-like transfer characteristics with no current flow under reverse bias and a noticeable increase in current at $V_{on} \sim +4.5$ V in forward bias. The G-PFCNC OLEDs gave an emission profile comparable to standard polyfluorene devices (Figure 5). Both emit blue colors, and most remarkably the presence of CNCs in the active layer does not tremendously alter the emissive properties of polyfluorene. Lowered emission intensities can be attributed to a difference in polyfluorene content. Emission peaks are realized at similar wavelengths in both the composite and standard material. Peaks at 422, 484, and 516 nm correspond to violet, blue, and cyan emissions in both devices and only one peak at 444 nm in the PF standard is less pronounced in the gPFCNC composite. Once again, this may be attributed to a lowered PF content in the composite material device. As both OLEDs are fabricated largely in air, except for thermal evaporation of metal electrodes, green shifted emissions may be the result of excimer formation or oxidation of the 9 position on fluorene units imparting a fluorenone group instead of the expected dialkyl chains^{28,36}.

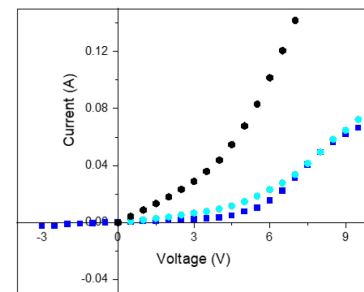


Figure 4. I-V curve sweep of polyfluorene standard (blue), polyfluorene with HTPA above (cyan), gPFCNC with HTPA above (black).

Based on the nonuniformity and thickness of the composite active layer, conventional wisdom would deem these devices as non-functional. In fact, a device fabricated with the most basic structure, glass/ITO/PEDOT:PSS/g-PFCNC/Ca/Al, does not operate. This could lead one to believe that the grafted composite material is not an effective semiconductor. Interestingly, emission only occurs when the HTPA electron blocking hole transport layer is present and layered above the composite active

layer. Without this hole transporting layer, the devices fail via short circuiting³⁹. When the HTPA encapsulation layer is employed, blue light is emitted beyond V_{on} . We hypothesize that the HTPA layer provides two benefits. The first is the filling of holes in the active layer that come about because of the intrinsically non-uniform film casting nature of gPFCNC. Being an insoluble material suspended in organic solvent, there is no observed self-assembly characteristic of pristine CNC films casted from water. Second, the HTPA aides in blocking electrons while transporting holes, reducing short circuiting phenomena that are seen in the absence of HTPA in these devices.

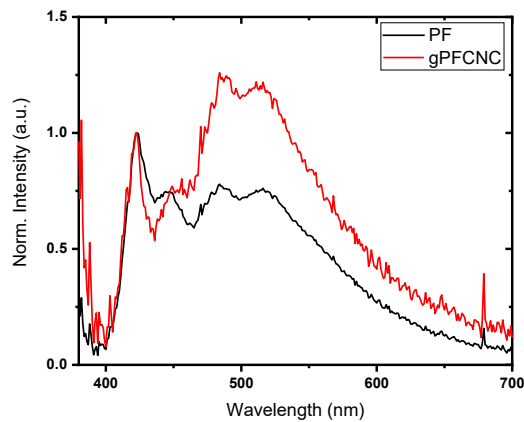


Figure 5. Normalized emission spectra of PF (black) and gPFCNC (red) shown over the visible wavelengths 380 – 700 nm.

In conclusion, we have synthesized a novel, emissive material using polyfluorene grafted from cellulose nanocrystals. Grafted chains were determined to be above the necessary effective conjugation length ($n \sim 10$) of poly (9,9-dihexylfluorene). Compared to previously reported grafting procedures, an increase of about 4x chain length was observed when utilizing Yamamoto-type Ni(0) mediated coupling chemistry. OLED devices were fabricated and demonstrated blue wavelength emission, characteristic of polyfluorene emitters. This work marks the beginnings of a future in emissive cellulosic composites. Along with paper substrate electronics, these emissive materials will aide researchers in the quest for more sustainably built, advanced electronic devices.

REFERENCES

- (1) Zhang, H.; Huang, L.; Zhai, J.; Dong, S. *Journal of the American Chemical Society*. Water/Oxygen Circulation-Based Biophotovoltaic System for Solar Energy Storage and Release. **2019**, *141*, 16416. DOI: 10.1021/jacs.9b08046
- (2) Cséfalvay, E.; Horváth, I. T. *ACS Sustainable Chemistry & Engineering*. Sustainability Assessment of Renewable Energy in the United States, Canada, the European Union, China, and the Russian Federation. **2018**, *6*, 8868. DOI: 10.1021/acssuschemeng.8b01213
- (3) Hu, B.; DeBruler, C.; Rhodes, Z.; Liu, T. L. *Journal of the American Chemical Society*. Long-Cycling Aqueous Organic Redox Flow Battery (AORFB) toward Sustainable and Safe Energy Storage. **2017**, *139*, 1207. DOI: 10.1021/jacs.6b10984
- (4) Luo, J.; Hu, B.; Hu, M.; Zhao, Y.; Liu, T. L. *ACS Energy Letters*. Status and Prospects of Organic Redox Flow Batteries toward Sustainable Energy Storage. **2019**, *4*, 2220. DOI: 10.1021/acsenergylett.9b01332
- (5) Best Research-Cell Efficiency Chart | Photovoltaic Research | NREL.
- (6) Green, M. A.; Dunlop, E. D.; Hohlebinger, J.; Yoshita, M.; Kopidakis, N.; Hao, X. *Progress in Photovoltaics: Research and Applications*. Solar cell efficiency tables (version 56). **2020**, *28*, 629. DOI: 10.1002/pip.3303
- (7) Bhuwalka, A.; Ewan, M. D.; Elshobaki, M.; Mike, J. F.; Tlach, B.; Chaudhary, S.; Jeffries-El, M. *Journal of Polymer Science Part A: Polymer Chemistry*. Synthesis and photovoltaic properties of 2,6-bis(2-thienyl) benzobisazole and 4,8-bis(thienyl)-benzo[1,2-B:4,5-B']dithiophene copolymers. **2016**, *54*, 316. DOI: 10.1002/pola.27793
- (8) Burney-Allen, A.; Shaw, J.; Wheeler, D.; Diodati, L.; Duzhko, V.; Tomlinson, A.; Jeffries-El, M. *Asian Journal of Organic Chemistry*. Benzobisoxazole cruciforms: A cross-conjugated platform for designing tunable donor/acceptor materials. **2020**, *n/a*. DOI: 10.1002/ajoc.202000502
- (9) Choi, D.; Chu, P.-H.; McBride, M.; Reichmanis, E. *Chemistry of Materials*. Best Practices for Reporting Organic Field Effect Transistor Device Performance. **2015**, *27*, 4167. DOI: 10.1021/acs.chemmater.5b01982
- (10) Wolfberger, A.; Petritz, A.; Fian, A.; Herka, J.; Schmidt, V.; Stadlober, B.; Kargl, R.; Spirk, S.; Griesser, T. *Cellulose*. Photolithographic patterning of cellulose: a versatile dual-tone photoresist for advanced applications. **2015**, *22*, 717. DOI: 10.1007/s10570-014-0471-4
- (11) Martins, R.; Gaspar, D.; Mendes, M. J.; Pereira, L.; Martins, J.; Bahubalindruni, P.; Barquinha, P.; Fortunato, E. *Applied Materials Today*. Papertronics: Multigate paper transistor for

multifunction applications. **2018**, *12*, 402. DOI: <https://doi.org/10.1016/j.apmt.2018.07.002>

(12) Wang, X.; Yu, C. *Journal of Materials Research*. Flexible low-voltage paper transistors harnessing ion gel/cellulose fiber composites. **2019**, *35*, 940. DOI: 10.1557/jmr.2019.303

(13) Risteen, B.; McBride, M.; Gonzalez, M.; Khau, B.; Zhang, G.; Reichmanis, E. *ACS Applied Materials & Interfaces*. Functionalized Cellulose Nanocrystal-Mediated Conjugated Polymer Aggregation. **2019**, *11*, 25338. DOI: 10.1021/acsmami.9b06072

(14) Min, S. H.; Kim, C. K.; Lee, H. N.; Moon, D. G.; Taylor & Francis Group; Vol. 563, p 159.

(15) Gomez, E. F.; Steckl, A. J. *ACS Photonics*. Improved performance of OLEDs on cellulose/epoxy substrate using adenine as a hole injection layer. **2015**, *2*, 439. DOI: 10.1021/ph500481c

(16) Lang, A. W.; Österholm, A. M.; Reynolds, J. R. *Advanced Functional Materials*. Paper-Based Electrochromic Devices Enabled by Nanocellulose-Coated Substrates. **2019**, *29*, 1903487. DOI: 10.1002/adfm.201903487

(17) Carlmark, A.; Malmström, E. *Journal of the American Chemical Society*. Atom Transfer Radical Polymerization from Cellulose Fibers at Ambient Temperature. **2002**, *124*, 900. DOI: 10.1021/ja016582h

(18) Lindqvist, J.; Nyström, D.; Östmark, E.; Antoni, P.; Carlmark, A.; Johansson, M.; Hult, A.; Malmström, E. *Biomacromolecules*. Intelligent Dual-Responsive Cellulose Surfaces via Surface-Initiated ATRP. **2008**, *9*, 2139. DOI: 10.1021/bm800193n

(19) Cao, X.; Habibi, Y.; Lucia, L. A. *Journal of Materials Chemistry*. One-pot polymerization, surface grafting, and processing of waterborne polyurethane-cellulose nanocrystal nanocomposites. **2009**, *19*, 7137. DOI: 10.1039/B910517D

(20) Habibi, Y. *Chemical Society Reviews*. Key advances in the chemical modification of nanocelluloses. **2014**, *43*, 1519. DOI: 10.1039/C3CS60204D

(21) Habibi, Y.; Goffin, A.-L.; Schiltz, N.; Duquesne, E.; Dubois, P.; Dufresne, A. *Journal of Materials Chemistry*. Bionanocomposites based on poly(ϵ -caprolactone)-grafted cellulose nanocrystals by ring-opening polymerization. **2008**, *18*, 5002. DOI: 10.1039/B809212E

(22) Klemm, D.; Heublein, B.; Fink, H.-P.; Bohn, A. *Angewandte Chemie International Edition*. Cellulose: Fascinating Biopolymer and Sustainable Raw Material. **2005**, *44*, 3358. DOI: 10.1002/anie.200460587

(23) Klemm, D.; Kramer, F.; Moritz, S.; Lindström, T.; Ankerfors, M.; Gray, D.; Dorris, A. *Angewandte Chemie International Edition*. Nanocelluloses: A New Family of Nature-Based Materials. **2011**, *50*, 5438. DOI: 10.1002/anie.201001273

(24) Zoppe, J. O.; Xu, X.; Kanel, C.; Orsolini, P.; Siqueira, G.; Tingaut, P.; Zimmermann, T.; Klok, H. A. *Biomacromolecules*. Effect of Surface Charge on Surface-Initiated Atom Transfer Radical Polymerization from Cellulose Nanocrystals in Aqueous Media. **2016**, *17*, 1404. DOI: 10.1021/acs.biomac.6b00011

(25) Zoppe, J. O.; Dupire, A. V. M.; Lachat, T. G. G.; Lemal, P.; Rodriguez-Lorenzo, L.; Petri-Fink, A.; Weder, C.; Klok, H.-A. *ACS Macro Letters*. Cellulose Nanocrystals with Tethered Polymer Chains: Chemically Patchy versus Uniform Decoration. **2017**, *6*, 892. DOI: 10.1021/acsmacrolett.7b00383

(26) Andrew R. Davis, K. R. C. *Langmuir*. Surface Grafting of Vinyl-Functionalized Poly(fluorene)s via Thiol-Ene Click Chemistry. **2014**, *30*, 4427–4433. DOI: 10.1021/la5000588

(27) Beinhoff, M.; Appapillai, A. T.; Underwood, L. D.; Frommer, J. E.; Carter, K. R. *Langmuir*. Patterned Polyfluorene Surfaces by Functionalization of Nanoimprinted Polymeric Features. **2006**, *22*, 2411. DOI: 10.1021/la051878c

(28) Bliznyuk, V. N.; Carter, S. A.; Scott, J. C.; Klärner, G.; Miller, R. D.; Miller, D. C. *Macromolecules*. Electrical and Photoinduced Degradation of Polyfluorene Based Films and Light-Emitting Devices. **1999**, *32*, 361. DOI: 10.1021/ma9808979

(29) Carter, A. R. D. a. K. R. *Macromolecules*. Controlling Optoelectronic Behavior in Poly(fluorene) Networks Using Thiol-Ene Photo-Click Chemistry. **2015**, *48*, 1711–1722. DOI: 10.1021/ma5014226

(30) Chang, A. C.; Chen, S.; Carter, K. R. *Cellulose*. Cellulose nanocrystal surface

modification via grafting-from sonogashira coupling of poly(ethynylene-fluorene). **2018**, *25*, 5731. DOI: 10.1007/s10570-018-1959-0

(31) Davis, A. R.; Carter, K. R. *Macromolecules*. Controlling Optoelectronic Behavior in Poly(fluorene) Networks Using Thiol-Ene Photo-Click Chemistry. **2015**, *48*, 1711. DOI: 10.1021/ma5014226

(32) Geng, Y.; Trajkovska, A.; Katsis, D.; Ou, J. J.; Culligan, S. W.; Chen, S. H. *Journal of the American Chemical Society*. Synthesis, Characterization, and Optical Properties of Monodisperse Chiral Oligofluorenes. **2002**, *124*, 8337. DOI: 10.1021/ja026165k

(33) Harris, J. D.; Liu, J.; Carter, K. R. *Macromolecules*. Synthesis of π -Bridged Dually-Dopable Conjugated Polymers from Benzimidazole and Fluorene: Separating Sterics from Electronics. **2015**, *48*, 6970. DOI: 10.1021/acs.macromol.5b01174

(34) Hwang, D.-H.; Kim, S.-K.; Park, M.-J.; Lee, J.-H.; Koo, B.-W.; Kang, I.-N.; Kim, S.-H.; Zyung, T. *Chemistry of Materials*. Conjugated Polymers Based on Phenothiazine and Fluorene in Light-Emitting Diodes and Field Effect Transistors. **2004**, *16*, 1298. DOI: 10.1021/cm035264+

(35) Lee, S. H.; Nakamura, T.; Tsutsui, T. *Organic Letters*. Synthesis and Characterization of Oligo(9,9-dihexyl-2,7-fluorene ethynylene)s: For Application as Blue Light-Emitting Diode. **2001**, *3*, 2005. DOI: 10.1021/ol010069r

(36) Zojer, E.; Pogantsch, A.; Hennebicq, E.; Beljonne, D.; Brédas, J.-L.; Scanducci de Freitas, P.; Scherf, U.; List, E. J. W. *The Journal of Chemical Physics*. Green emission from poly(fluorene)s: The role of oxidation. **2002**, *117*, 6794. DOI: 10.1063/1.1507106

(37) Peterson, J. J.; Willgert, M.; Hansson, S.; Malmström, E.; Carter, K. R. *Journal of Polymer Science Part A: Polymer Chemistry*. Surface-Grafted conjugated polymers for hybrid cellulose materials. **2011**, *49*, 3004. DOI: 10.1002/pola.24733

(38) Hai, T. A. P.; Sugimoto, R. *Carbohydrate Polymers*. Surface functionalization of cellulose with poly(3-hexylthiophene) via novel oxidative polymerization. **2018**, *179*, 221. DOI: <https://doi.org/10.1016/j.carbpol.2017.09.067>

(39) Bozano, L. D.; Carter, K. R.; Lee, V. Y.; Miller, R. D.; DiPietro, R.; Scott, J. C. *Journal of Applied Physics*. Electroluminescent devices based on cross-linked polymer blends. **2003**, *94*, 3061. DOI: 10.1063/1.1599625